Title

A phantom based evaluation of vessel lumen area quantification for coronary CT angiography

Journal

The International Journal of Cardiovascular Imaging, 35(3)

ISSN

1569-5794

Authors

Molloi, Sabee
Johnson, Travis
Lipinski, Jerry
et al.

Publication Date

2019-03-01

DOI

10.1007/s10554-018-1452-8

Peer reviewed

HHS Public Access

Author manuscript

Int J Cardiovasc Imaging. Author manuscript; available in PMC 2020 March 01.

Published in final edited form as:

Int J Cardiovasc Imaging. 2019 March ; 35(3): 551–557. doi:10.1007/s10554-018-1452-8.

A phantom based evaluation of vessel lumen area quantification for coronary CT angiography

Sabee Molloi[1,2], **Travis Johnson**[1], **Jerry Lipinski**[1], **Huanjun Ding**[1], **Logan Hubbard**[2]

[1]Department of Radiological Sciences, Medical Sciences B, 140, University of California, Irvine, CA 92697, USA

[2]Department of Biomedical Engineering, University of California, Irvine, CA 92697, USA

Abstract

Coronary computed tomography (CT) angiography is a noninvasive method for visualizing coronary artery disease. However, coronary CT angiography is limited in assessment of stenosis severity by the partial volume effect and calcification. Therefore, an accurate method for assessment of stenosis severity is needed. A 10 cm diameter cylindrical Lucite phantom with holes in the range of 0.4–4.5 mm diameter was fitted in a chest phantom. The holes were filled with an iodine solution of 8 mg/mL. To simulate coronary artery disease, different levels of stenosis were created by inserting Lucite rods into the holes with diameter range of 2–4.5 mm. The resulting lumen cross sectional areas ranged from 1.4 to 12.3 mm^2. To simulate arterial calcification, calcium hydroxyapatite rods were inserted into the holes with diameter range of 2–4.5 mm. Images of the phantoms were acquired at 100 kVp using a 320-slice CT scanner. A maual and a semi-automated technique based on integrated Hounsfield units was used to calculate vessel cross-sectional area. There was an excellent correlation between the measured and the known cross-sectional area for both normal and stenotic vessels using the manual and the semi-automated techniques. However, the overall measurement error for the manual method was more than twice as compared with the integrated HU technique. Determination of vessel lumen area using the semi-automated integrated Hounsfield unit technique yields more than a factor of two improvement in precision and accuracy as compared to the existing manual technique for vessels with and without stenosis. This technique can also be used to accurately measure arterial cross-sectional area in the presence of coronary calcification.

Keywords

Computed tomography; Angiography; Coronary artery disease; Imaging

Introduction

Coronary CT angiography (CTA) has now become an established method of evaluating patients with suspected coronary artery disease [1–3]. The method is suitable for excluding the presence of coronary atherosclerosis. However, previous CT angiography studies have

symolloi@uci.edu.

observed an overestimation of stenosis severity [4, 5]. Previous reports indicate that CT angiography inaccurately identifies coronary lesions as severe and the identified lesions are the actual cause of ischemia less than one-half of the time [5]. This finding has led to concerns that widespread application of CT angiography may result in unnecessary invasive coronary angiography [6].

Accurate measurement of vessel lumen area is limited by low spatial resolution and the partial volume effect. Existing techniques for lumen area measurement are particularly limited for vessels with small lumen area, which includes the stenotic region. Partial volume effect limits the accurate visualization and measurement of stenosis severity. There have been previous efforts to improve the visualization of a stenotic vessel by displaying the images with a standard window and level [7–9].

Another major limitation of coronary CT angiography is the presence of severe arterial calcification and implanted stents, which substantially reduces its diagnostic accuracy [10]. They cause blooming artifacts that hamper visualization of stenosis. As coronary calcification is relatively common in patients with chest pain syndromes in need of diagnostic work-up, this can lead to a large fraction of patients referred for coronary CT angiography [11].

There have been previous efforts to measure lumen area in the presence of calcification by subtracting a pre-contrast image to eliminate the calcification [12]. However, accuracy of the subtraction technique is highly limited by motion artifacts that are difficult to correct. Furthermore, accurate coronary lesion lumen area has been shown to be one of the most important input parameters for accurate estimation of CT-based fractional flow reserve (FFR) using flow simulation [13]. There is a clear need for an automated technique to accurately measure lumen area in the presence of stenosis and calcification.

We have previously reported the results of a computer simulation study using an integrated HU technique for accurate measurement of vessel lumen area [14]. In this paper we have validated the integrated HU technique in physical phantoms with stenosis and calcification where the lumen area is known in order to explore its efficacy.

Materials and methods

Lumen area measurement using integrated HU technique

In order to account for the partial volume effect, we have developed an integrated HU based approach for lumen area measurement. The assumption is that, although the HU of a certain voxel is influenced by the partial volume effect, the total integrated HU within a region of interest (ROI) is conserved. The concept behind this method is shown in Fig. 1, which shows a vessel phantom inside a chest phantom with two materials: high HU iodine solution within the vessel lumen and relatively lower HU of the stenotic material and vessel wall. We use three ROIs: (1) a central calibration ROI which includes only pixels that are unaffected by the partial volume effect to measure the true HU in the lumen (S_O), (2) an object ROI which includes the entire iodine signal in the lumen, including any voxels that are affected by the partial volume effect, and (3) a ring ROI just outside the object ROI to measure the

background HU (S_{BG}). The integrated HU (I) measured from the object ROI includes partial volume effect. However, using the above assumption about signal conservation, it is the same as the integrated signal without the partial volume effect and can be written as:

$$I = (A - CSA) \times S_{BG} + CSA \times S_O \quad (1)$$

where A is the total area of object ROI. Hence, lumen area (CSA) can be derived as:

$$CSA = \frac{I - A \times S_{BG}}{S_O - S_{BG}} \quad (2)$$

The proposed lumen area measurement technique does not directly depend on the spatial resolution of an imaging system since the integrated HU is used for lumen area measurement rather than the vessel dimension. It is capable of quantifying a small lumen area despite the partial volume effect.

Phantom measurements

A 10 cm diameter cylindrical Lucite phantom with holes in the range of 0.4–4.5 mm diameter was fitted in a chest phantom (Quality Assurance in Radiology and Medicine, Moehrendorf, Germany). The holes were filled with an iodine solution of 8 mg/mL to create a contrast of approximately 380 HU relative to the background. To simulate disease, different levels of stenosis were created by inserting Lucite cylindrical rods into the holes with diameters in the range of 2–4.5 mm. The resulting lumen cross sectional areas ranged from 1.4 to 12.3 mm^2. To simulate arterial calcification, calcium hydroxyapatite cylindrical rods were inserted into the holes with diameters in the range of 2–4.5 mm. The resulting lumen cross sectional areas ranged from 4 to 14 mm^2. Images of the phantoms were acquired at 100 kVp with an equivalent $CTDI_{vol}$ of 5.6 mGy (see Fig. 1) using a 320-slice CT scanner (Aquilion One, Toshiba American Medical Systems, Tustin, CA). CT images were reconstructed with a slice thickness of 0.5 mm using a medium smooth FC03 kernel with beam hardening corrections. The voxel size was 0.43 × 0.43 × 0.5 mm^3.

The integrated HU technique can also be used applied when there are additional materials near the vessel. We evaluated its performance in the presence of a calcification using pre- and post-contrast images to account for the integrated HU due to calcification. In the presence of calcification or other materials such as implanted stent, Eq. (2) above can be modified to account for its integrated HU. The lumen area in the presence of calcification can be written as:

$$CSA = \frac{\left(\left(I - I_{Ca}\right) - A \times S_{BG}\right)}{S_O - S_{BG}} \quad (3)$$

where I_{ca} is the integrated HU in the pre-contrast image with calcification. We have assumed that the size of the object ROI (A) and the background (S_{BG}) are the same for the pre- and post-contrast images. However, this is not a requirement since the integrated HU for the pre- and post-contrast images are measured separately. Therefore, the pre- and post-contrast images do not necessarily need to be registered, which has important implications in the case of motion misregistration between the images.

Reader assessment of lumen area

All analysis was completed on a dedicated workstation with custom graphical user interface (GUI) software written in MATLAB. Vessels were presented in a random order with the constraint that realizations of the same vessel were separated by at least three images. Two trained readers performed lumen area measurements in the vessel phantoms with and without stenosis using hand-delineated ROIs with the GUI software [15]. Following a previous report, the display window and level were set automatically at 155% and 65% of the mean luminal enhancement, respectively [16]. However, readers were free to zoom and adjust the display settings for better visualization, especially for small vessels where the partial volume effect greatly reduced the lumen HU.

The object ROIs for the integrated HU technique was first automatically generated by region growing within the lumen of the vessels, and then adjusted manually to ensure the inclusion of the entire lumen with contrast material. Once the object ROIs were determined, the ring ROIs were automatically drawn concentrically using expansion that was 1.2 times larger than that of the object ROIs. One calibration ROI was concentric with a large vessel to measure the true contrast HU without the partial volume effect. The mean pixel values and areas of these three ROIs were recorded automatically and used for lumen area calculation using Eqs. (2) or (3).

Statistical analyses

The root-mean-square (RMS) deviations from the fit and the RMS errors to the known values were calculated to assess the precision and accuracy of the measurement, respectively. Reliability of the lumen area measurements was evaluated using the coefficient of variation (CV). The coefficient of variation was computed from the independent realizations of each vessel by taking the ratio of the standard deviation over the mean.

Results

Figures 2 and 3 show the lumen area measurements of the vessels without stenosis performed by two readers and the semi-automated integrated HU technique, respectively. The lumen area measurement results from the two readers show a relatively large intra-observer and inter-observer variability (Fig. 2). The variability in lumen area measurement was substantially reduced with the integrated HU technique (Fig. 3).

Figures 4 and 5 show the lumen area measurements of the vessels with stenosis performed by two readers and the semi-automated integrated HU technique, respectively. There was a substantial increase in intra-observer and inter-observer variability in lumen area measurement for the two readers in vessels with stenosis as compared to vessels without

stenosis (Fig. 4). This is due to the more complex crescentic lumen area of the stenosis vessels as compared with the normal circular lumen area for normal vessels. On the other hand, the variability in lumen area measurement by the integrated HU technique only slightly increased for stenosis vessels as compared with the normal vessels (Fig. 5). The slight increase in variability is due to the fact that drawing ROIs for crescentic lumen area stenosis vessels is more difficult than the normal circular lumen area.

Tables 1 and 2 show a summary of the linear regression parameters, RMS deviation and RMS error for the vessels with and without stenosis. Figure 6 shows a comparison of precision (RMS deviation) and accuracy (RMS error) for vessels with and without stenosis. Although a good correlation was found in the manual method, the overall RMS error was approximately twice as large as the result from the integrated HU technique for vessels without stenosis and three times as large for vessels with stenosis. Figure 7 shows the coefficient of variation for the integrated HU method and the two readers in the vessels without stenosis. The coefficient of variation was higher than 10% for vessel lumen areas less than 12 and 2 mm^2 for the readers and the integrated HU technique, respectively. The increase in coefficient of variation for the integrated HU technique for lumen areas less than 2 mm^2 indicates that the technique is ultimately limited by the low signal to noise for the very small lumen areas.

It is also possible to measure lumen area in the presence of arterial calcification. Pre- and post-contrast images were used to account for the integrated HU from calcification. The integrated HU in the object ROI from the pre-contrast image was measured and then subtracted from the independently measured integrated HU of the post-contrast image to account for the integrated HU from calcification. Figure 8 shows the lumen area measurement results after correction for the integrated HU from calcification. The measured lumen area is in good agreement with the known lumen area. This indicates that the pre-contrast images can be used to account for the measured integrated HU from calcification in the post-contrast image, which enables accurate lumen area measurement in the presence of calcification.

Discussion

Our measurement results in physical phantoms show that the integrated HU can be used to accurately measure vessel lumen area by accounting for the partial volume effect. The results of our semi-automated technique show that it can improve the precision and accuracy of vessel lumen area as compared with the existing manual technique. The integrated HU technique showed approximately a factor of two improvement in precision and accuracy for vessels without stenosis. It showed more than a factor of two improvement in precision and more than a factor of three improvement in accuracy for vessels with stenosis. This is particularly true in the case of small vessel diameters where the lumen area measurement is more limited by partial volume effect. The coefficient of variation for lumen area measurements using the integrated HU technique in vessels without stenosis was less than 10% for lumen area greater than 2 mm^2 while for the existing manual technique this lumen area was more than 12 mm^2. This shows a substantial reduction in variability of lumen area measurement for small vessel diameters using the integrated HU technique. Our results show

that there was a large variability between different readers. This inter-observer variability is essentially eliminated with the integrated HU technique.

The integrated HU technique requires determination of the mean HU inside and outside the vessel lumen, which is unaffected by partial volume effect for accurate measurement of vessel lumen area. This can be accomplished by measuring the mean HU at the center of the lumen and away from the vessel wall so it will not be affected by the partial volume effect. However, in the case of a stenosis, the HU inside the lumen can be entirely affected by partial volume effect. Therefore, in the case of a severe stenosis the unaffected HU can be estimated by averaging the HU in the normal lumen before and after the stenosis.

Coronary CT angiography has shown decreased diagnostic accuracy in the presence of severe calcification [17, 18]. The integrated HU technique uses a pre-contrast image to measure the integrated HU due to calcification. The pre- and post-contrast integrated HU are then subtracted to account for the effect of calcification. The integrated HU measurements are done independently in the pre- and post-contrast images so the technique is immune to motion misregistration artifacts. The results show that the integrated HU technique in conjunction with a pre-contrast image can be used to accurately measure lumen area even in the presence of calcification. In fact, the precision and accuracy of lumen area measurement were approximately the same with or without calcification. A CT digital subtraction angiography technique has previously been reported to address the limitations of calcification in coronary CT angiography [12]. However, this technique works well only when there is good registration between the pre- and post-contrast scans. A previous report has indicated that misregistration artifacts were seen in approximately half of all target arterial segments [12]. In addition to calcification, the integrated HU technique is expected to also perform well in the presence of implanted stents using pre- and post-contrast images. Future in-vivo validation of the integrated HU technique are needed to assess its ability to accurately measure vessel lumen area in the presence of calcification and implanted stents.

It is important to point out that the lumen area measurement using the integrated HU technique does not use the number of voxels across a vessel for lumen area measurement, which is the approach for the standard techniques. It uses the difference in the integrated HU between the vessel lumen and the background for the measurement, which is more limited by contrast resolution than spatial resolution. This is particularly important in the case of a tight stenosis where the vessel lumen is difficult to detect using standard segmentation techniques. It is possible to accurately measure vessel lumen area as long as a difference in HU is measured as compared to the background even in the cases where the lumen is difficult to detect.

Coronary CT angiography image data has recently been used to derive fractional flow reserve (FFR) to estimate the physiological severity of a stenosis [19–21]. In this approach, the geometrical parameters of the stenosis and arterial tree are used to perform computational fluid dynamics and estimate pressure drop across the stenosis [19–21]. A previous report has shown that lesion lumen area and flow rate are the most important parameters for accurate estimation of FFR based on stenosis geometrical parameters [13].

Therefore, accurate measurement of lesion lumen area is expected to also improve existing techniques for estimation of FFR based on CT angiography.

The integrated HU technique assumes uniform material densities inside and outside the lumen, which might introduce some error in lumen area measurement for in-vivo applications. The mean HU inside and outside the lumen was estimated using a large region of interest inside and a ring region of interest outside the lumen to minimize any potential error in lumen area estimation. However, large variation in HU close to vessel lumen can potentially introduce error in lumen area estimation. It is expected that calcification and stent will produce large variation in HU close to vessel wall, which will require a pre-contrast image at the same imaging parameters for accurate lumen area measurement. Finally, accurate lumen area measurement in the presence of calcification will require a registered pre-contrast image. The integrated HU technique is immune to any motion of calcification within a slice but image registration is needed to correct any motion in or out of a slice. This is particularly true in the case of large changes in calcification HU along the vessel length. Therefore, large motion between the pre- and post-contrast images that are not corrected during 3D image registration can potentially introduce error in lumen area measurement.

This study has a number of potential limitations. The integrated HU technique was tested using a standard chest phantom. Although the accuracy of the technique is not expected to be affected by the patient chest size, future studies will need to evaluate the technique for different chest sizes. This study did not consider cardiac and respiratory motion artifacts. However, motion artifacts are not expected to affect the lumen area measurement as long as the background ROI does not include any iodine signal from the lumen. In other words, the integrated iodine signal from the vessel lumen is not expected to change with motion. However, it is expected to be more challenging to automatically detect and place ROIs in a case of a blurred vessel. Uniform shaped Lucite rods were used to simulate arterial stenosis and calcification. An actual stenosis can have any irregular shape with blurred interface between contrast medium and the vessel wall, which will also be challenging to automatically detect and place ROIs. However, as long as the integrated iodine signal and the vessel wall or calcification could be separated, accurate vessel lumen area measurement is expected.

In conclusion, determination of vessel lumen area using the semi-automated integrated Hounsfield unit technique yields more than a factor of two improvements in precision and accuracy as compared to the existing manual technique for vessels with and without stenosis. This technique can also be used to correct for the effect of coronary calcification.

Acknowledgements

The authors would like to thank Ms. Rachel Smith for her help with data analysis. This work was supported in part by a Grant from Canon America Medical System Inc.

Conflict of interest S. Molloi has received grant funding from Canon America Medical System Inc.

References

1. Achenbach S, Daniel WG (2001) Noninvasive coronary angiography—an acceptable alternative? N Engl J Med 345(26):1909–1910 [PubMed: 11756583]
2. Budoff MJ et al. (2008) Diagnostic performance of 64-multi-detector row coronary computed tomographic angiography for evaluation of coronary artery stenosis in individuals without known coronary artery disease: results from the prospective multicenter ACCURACY (Assessment by Coronary Computed Tomographic Angiography of Individuals Undergoing Invasive Coronary Angiography) trial. J Am Coll Cardiol 52(21):1724–1732 [PubMed: 19007693]
3. Min JK, Shaw LJ, Berman DS (2010) The present state of coronary computed tomography angiography a process in evolution. J Am Coll Cardiol 55(10):957–965 [PubMed: 20202511]
4. Goldstein JA et al. (2007) A randomized controlled trial of multi-slice coronary computed tomography for evaluation of acute chest pain. J Am Coll Cardiol 49(8):863–871 [PubMed: 17320744]
5. Meijboom WB et al. (2008) Comprehensive assessment of coronary artery stenoses: computed tomography coronary angiography versus conventional coronary angiography and correlation with fractional flow reserve in patients with stable angina. J Am Coll Cardiol 52(8):636–643 [PubMed: 18702967]
6. Nissen SE (2008) Limitations of computed tomography coronary angiography. J Am Coll Cardiol 52(25):2145–2147 [PubMed: 19095131]
7. Marwan M et al. (2011) Coronary vessel and luminal area measurement using dual-source computed tomography in comparison with intravascular ultrasound: effect of window settings on measurement accuracy. J Comput Assist Tomogr 35(1):113–118 [PubMed: 21245696]
8. Komatsu S et al. (2014) Quantitative analysis of coronary vessels with optimized intracoronary CT number. Plos One 9(1):e85312 [PubMed: 24409326]
9. Jiayin Z et al. (2015) Quantification of coronary artery stenosis by area stenosis from cardiac CT angiography. Conf Proc IEEE Eng Med Biol Soc 2015:695–698 [PubMed: 26736357]
10. Kruk M et al. (2014) Impact of coronary artery calcium characteristics on accuracy of CT angiography. JACC Cardiovasc Imaging 7(1):49–58 [PubMed: 24290567]
11. Miller JM et al. (2008) Diagnostic performance of coronary angiography by 64-row CT. N Engl J Med 359(22):2324–2336 [PubMed: 19038879]
12. Fuchs A et al. (2015) Feasibility of coronary calcium and stent image subtraction using 320-detector row CT angiography. J Cardiovasc Comput Tomogr 9(5):393–398 [PubMed: 26091841]
13. Huo Y et al. (2012) A validated predictive model of coronary fractional flow reserve. J R Soc Interface 9(71):1325–1338 [PubMed: 22112650]
14. Molloi S et al. (2017) Accurate quantification of vessel cross-sectional area using CT angiography: a simulation study. Int J Cardiovasc Imaging 33(3):411–419 [PubMed: 27838897]
15. Rasband WS (1997–2005) ImageJ. http://rsb.info.nih.gov/ij/
16. Leber AW et al. (2005) Quantification of obstructive and nonobstructive coronary lesions by 64-slice computed tomography: a comparative study with quantitative coronary angiography and intravascular ultrasound. J Am Coll Cardiol 46(1):147–154 [PubMed: 15992649]
17. Vavere AL et al. (2011) Coronary artery stenoses: accuracy of 64-detector row CT angiography in segments with mild, moderate, or severe calcification—a subanalysis of the CORE-64 trial. Radiology 261(1):100–108 [PubMed: 21828192]
18. Abdulla J et al. (2012) Influence of coronary calcification on the diagnostic accuracy of 64-slice computed tomography coronary angiography: a systematic review and meta-analysis. Int J Cardiovasc Imaging 28(4):943–953 [PubMed: 21667273]
19. Kim HJ et al. (2010) Patient-specific modeling of blood flow and pressure in human coronary arteries. Ann Biomed Eng 38(10):3195–3209 [PubMed: 20559732]
20. Koo BK et al. (2011) Diagnosis of ischemia-causing coronary stenoses by noninvasive fractional flow reserve computed from coronary computed tomographic angiograms. Results from the prospective multicenter DISCOVER-FLOW (Diagnosis of Ischemia-Causing Stenoses Obtained Via Noninvasive Fractional Flow Reserve) study. J Am Coll Cardiol 58(19):1989–1997 [PubMed: 22032711]

21. Min JK et al. (2012) Diagnostic accuracy of fractional flow reserve from anatomic CT angiography. JAMA 308(12):1237–1245 [PubMed: 22922562]

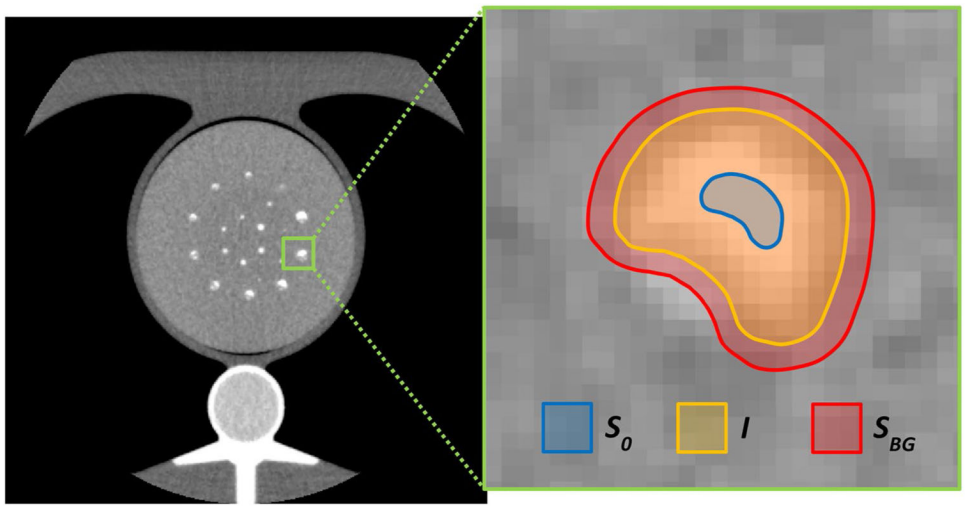

Fig. 1.

An example image of the vessel phantom without calcification inside a chest phantom is shown. An expansion of one vessel lumen is shown with ROIs for lumen area measurement where the central ROI that yields S_O and the background ROI that yields S_{BG} are unaffected by partial volume effect while the object ROI used to calculate I is affected by partial volume effect

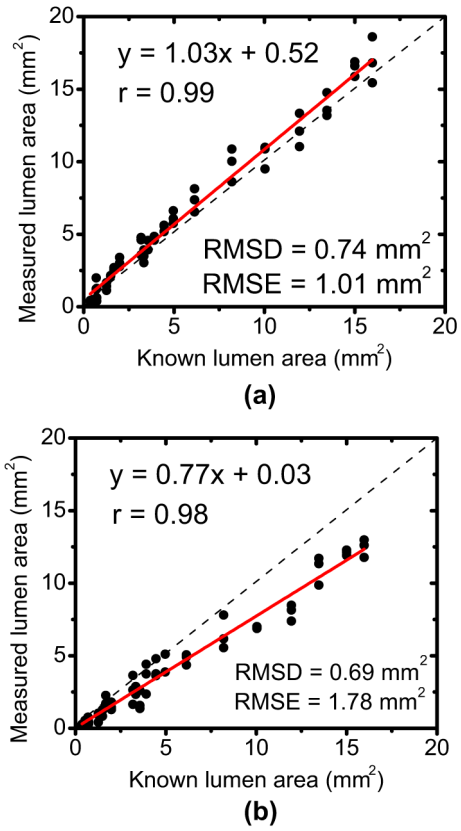

Fig. 2.

Linear regression analysis comparing measured lumen area by reader 1 (**a**) and reader 2 (**b**) to the known lumen area for vessels without stenosis. The best fit line, its equation and Pearson's r value are shown in each plot

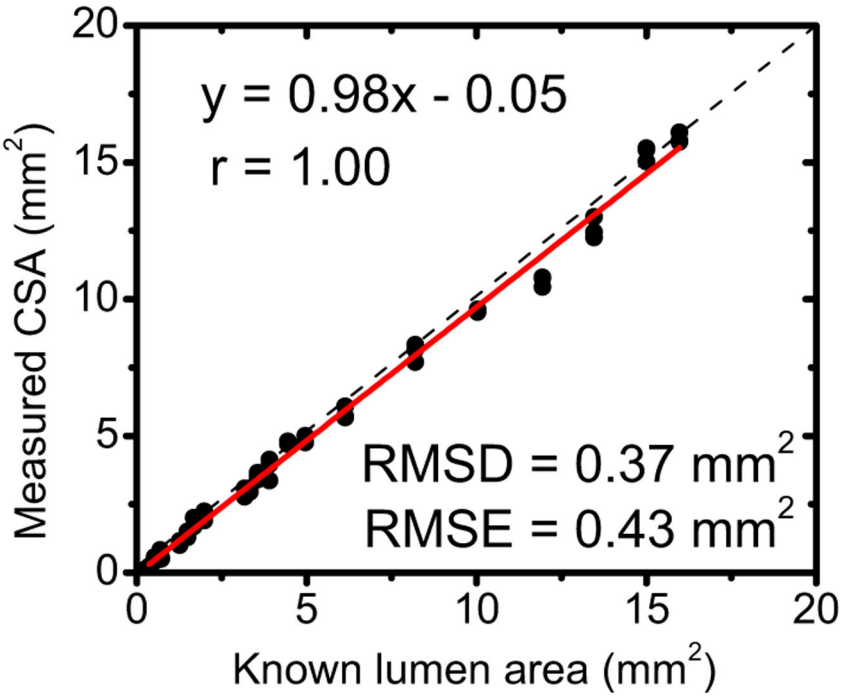

Fig. 3.

Linear regression analysis comparing measured lumen area using the integrated HU technique to the known lumen area for vessels without stenosis. The best fit line, its equation and Pearson's r value are shown

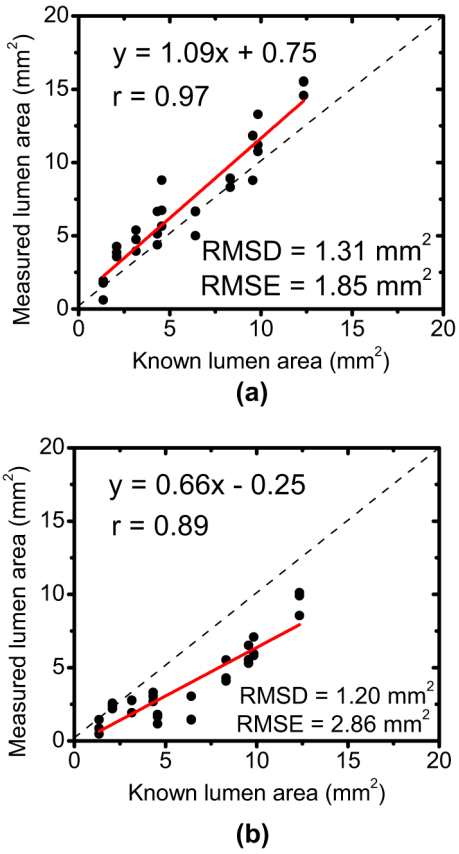

Fig. 4.

Linear regression analysis comparing measured lumen area by reader 1 (**a**) and reader 2 (**b**) to the known lumen area for vessels with stenosis. The best fit line, its equation and Pearson's r value are shown in each plot

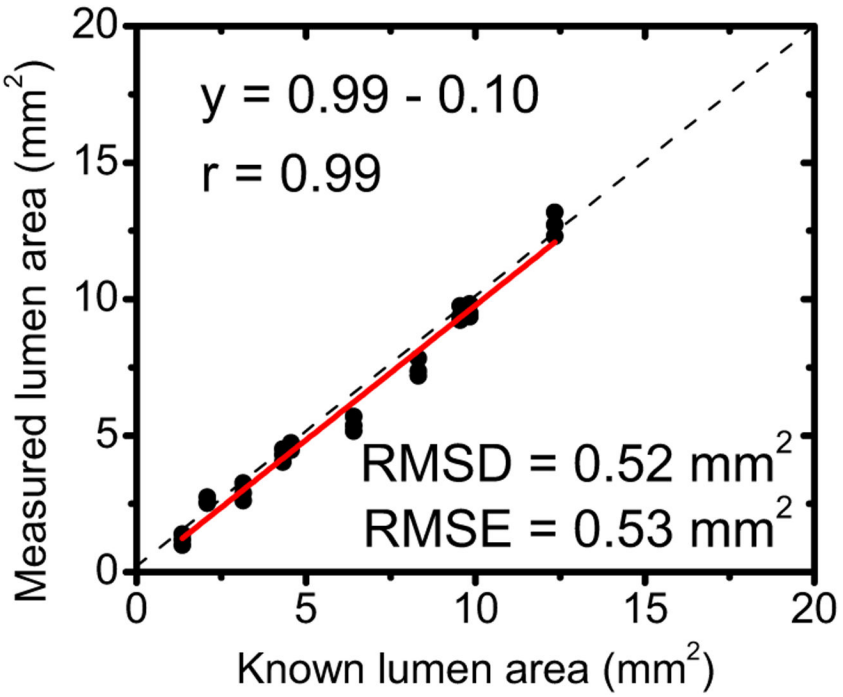

Fig. 5.

Linear regression analysis comparing measured lumen area using the integrated HU technique to the known lumen area for vessels with stenosis that do not include calcification. The best fit line, its equation and Pearson's r value are shown

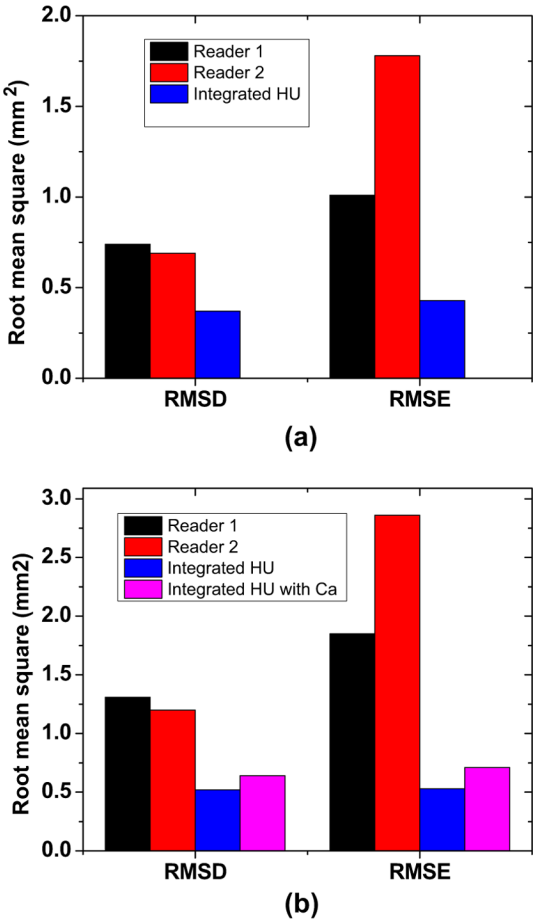

Fig. 6.

Comparisons of precision and accuracy quantified by the root-mean-square deviations from the best fit line (RMSD), and the root-mean-square errors to the known values (RMSE), respectively. The precision and accuracy were measured for vessels without stenosis (**a**) and vessels with stenosis that do not include calcification (**b**) for two readers and the integrated HU technique without and with calcification

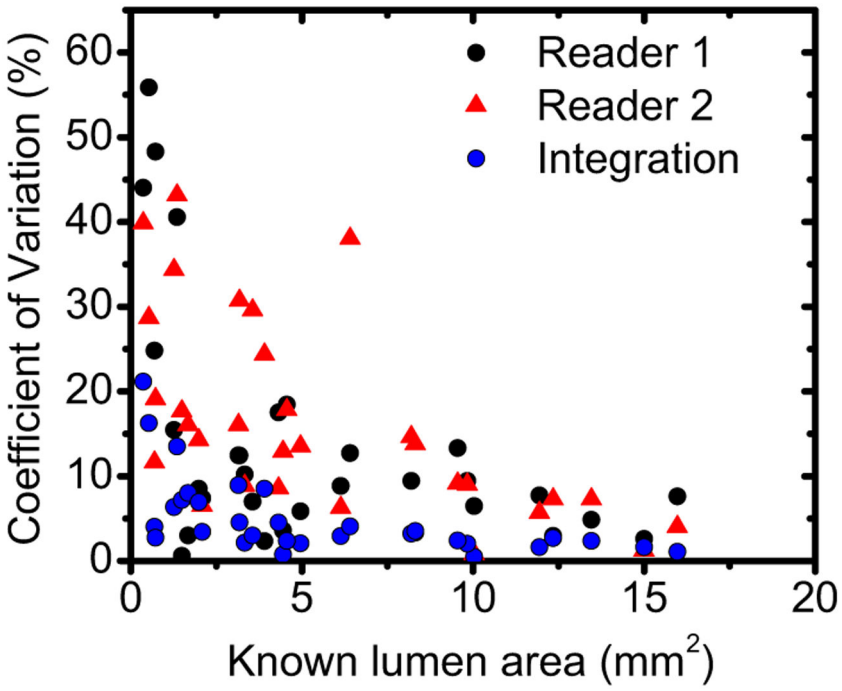

Fig. 7.

Reliability of the lumen area measurements for the readers and the integrated HU technique are compared using the coefficient of variation. The coefficient of variation is computed from the independent realizations of each vessel by taking the ratio of the standard deviation over the mean

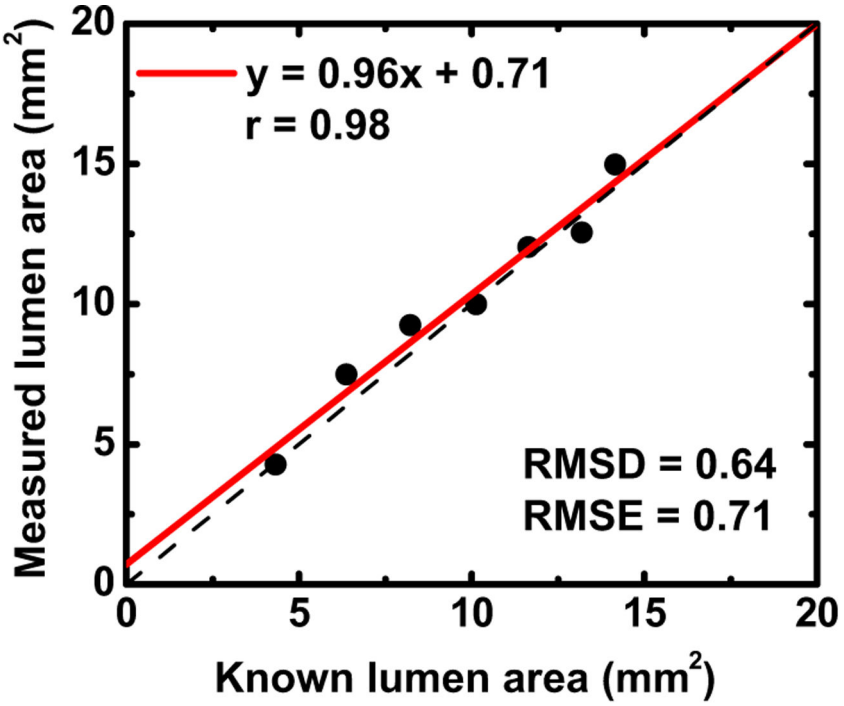

Fig. 8.

Correlation between measured and known lumen area with calcification. The best fit line, its equation and Pearson's r value are shown

Table 1

Summary of the linear regression analysis for the readers and the integrated HU technique in vessels without stenosis is shown

	Reader 1	Reader 2	Integrated HU
Slope	1.03	0.77	0.98
Intercept (mm^2)	0.52	0.03	−0.05
Pearson's r	0.99	0.98	1.00
RMSD (mm^2)	0.74	0.69	0.37
RMSE (mm^2)	1.01	1.78	0.43

The root mean square difference (RMSD) and the root mean square error (RMSE) represent precision and accuracy, respectively

Table 2

Summary of the linear regression analysis for the readers and the integrated HU technique in vessels with stenosis is shown

	Reader 1	Reader 2	Integrated HU	Integrated HU with calcification
Slope	1.09	0.66	0.99	0.96
Intercept (mm^2)	0.75	−0.25	−1.0	0.71
Pearson's r	0.97	0.89	0.99	0.98
RMSD (mm^2)	1.31	1.20	0.52	0.64
RMSE (mm^2)	1.85	2.86	0.53	0.71

The root mean square difference (RMSD) and the root mean square error (RMSE) represent precision and accuracy, respectively